Thin Solid Films xxx (2014) xxx–xxx

Contents lists available at ScienceDirect

Thin Solid Films

journal homepage: www.elsevier.com/locate/tsf

Determination of an optimal measurement configuration in optical scatterometry using global sensitivity analysis

Zhengqiong Dong [a], Shiyuan Liu [a,b,*], Xiuguo Chen [a], Chuanwei Zhang [b]

[a] Wuhan National Laboratory for Optoelectronics, Huazhong University of Science and Technology, Wuhan, Hubei, 430074, China
[b] State Key Laboratory of Digital Manufacturing Equipment and Technology, Huazhong University of Science and Technology, Wuhan, Hubei, 430074, China

ARTICLE INFO

Article history:
Received 3 June 2013
Received in revised form 26 February 2014
Accepted 16 March 2014
Available online xxxx

Keywords:
Optical scatterometry
Measurement configuration
Precision
Global sensitivity analysis
Uncertainty index
Local sensitivity analysis

ABSTRACT

In optical scatterometry, a proper measurement configuration has a significant impact on the precision of the reconstructed profile parameters beyond the quality of the measured signatures. In this paper, we propose to determine an optimal measurement configuration for optical scatterometry with the application of global sensitivity analysis (GSA). For each measurement configuration, we define a metric called the uncertainty index to evaluate the impact of random noise in measured signatures on measurement precision by combining the corresponding noise level with the main effect defined in GSA. Experiments performed on a one-dimensional silicon grating with its true dimensions close to its nominal values have revealed a trend that the lower the uncertainty index, the better the precision of the reconstructed profile parameters. This trend shows an agreement between the theoretically predicted and experimentally obtained optimal measurement configurations. The uncertainty index also predicts an optimal measurement configuration for a set of grating samples with various dimensions, which shows a similar trend in agreement with that by numerical simulations. In contrast, the optimal configuration predicted using the local sensitivity analysis method is significantly dependent on the nominal dimensions of the samples, and consequently it is difficult to achieve a proper configuration for all the investigated samples. The results suggest that the defined uncertainty index by the GSA method is suitable to determine an optimal measurement configuration, especially for a set of samples with relatively large dimensional variation.

1. Introduction

Recently, optical scatterometry has been widely used for critical dimension (CD) and overlay metrology in the semiconductor industry because it is fast, noncontact, nondestructive, and of low-cost compared to other techniques such as scanning electron microscopy (SEM) and atomic force microscopy [1–3]. As a model-based metrology, it involves both the forward modeling of sub-wavelength structures and the reconstruction of structural profiles from the measured signatures [4–6]; thus, it is a typical inverse problem with the objective of finding a modeled profile whose calculated signatures can best match the measured ones using regression analysis or library search [7,8]. Here, the general term 'signatures' contain the scattered light information from the diffractive grating structure, which can be in the form of reflectance, ellipsometric angles, Stokes vector elements, or Mueller matrix elements. The regression analysis or library search method optimizes a set of floating profile parameters (e.g., CD, side wall angle, and height) under a fixed measurement configuration, which is defined as a combination of selected wavelengths, incidence, and azimuthal angles [9]. In addition to the quality of the measured signatures, the measurement configuration also has a significant impact on the precision of the reconstructed profile parameters [10,11]. One method for improving precision is to enhance the quality of the instrument. Another method, also the focus of this research, is to determine an optimal measurement configuration that maximizes the sensitivity of the modeled signatures with respect to the variations of the profile parameters and at the same time minimizes the impact of the measurement noise on these reconstructed profile parameters.

Sensitivity analysis is a useful tool for qualitatively or quantitatively estimating the influence of the variations in model input profile parameters on the model output [12]. Currently, several approaches based on sensitivity analysis have been developed to determine an optimal measurement configuration for optical scatterometry. For example, Ku et al. conducted qualitative sensitivity analysis to select some feature regions containing all the possible incidence angles that yield the best sensitivity [13]. They proposed to reconstruct the profile parameters by seeking reflectance only in relatively few feature regions rather than in the full library, thus improving both the measurement precision and the measurement speed. Logofătu [14], Silver et al. [15], Foldyna et al. [16],

* Corresponding author at: State Key Laboratory of Digital Manufacturing Equipment and Technology, Huazhong University of Science and Technology, Wuhan, Hubei, 430074, China.
E-mail address: shyliu@mail.hust.edu.cn (S. Liu).

http://dx.doi.org/10.1016/j.tsf.2014.03.051
0040-6090/

and Germer et al. [17] performed statistical analysis to obtain the curvature matrix based on the partial derivatives of the modeled signatures with respect to the profile parameters over all the measurement configurations. The inverse of the curvature matrix is an estimate of the covariance matrix, and a minimization of the diagonal elements of the covariance matrix will optimize the measurement configuration for those corresponding profile parameters. Vagos et al. developed an uncertainty and sensitivity analysis package for guiding the model and azimuthal angle optimization processes [18]. In general, all the abovementioned approaches involve calculating the partial derivatives of the modeled signatures with respect to the profile parameters. This kind of partial derivative-based sensitivity analysis is usually called local sensitivity analysis (LSA), which examines the local response of the modeled signatures by varying one profile parameter by a small offset from its nominal value, while the others are fixed at their nominal values [19]. LSA has the advantage of being easy to conduct and is very efficient in reducing computational time. However, it cannot take into account the interactional influences among profile parameters on the model output and the local sensitivity index of a profile parameter is significantly affected by the fixed values of other parameters, when the model under analysis is non-linear.

In this paper, we propose to apply global sensitivity analysis (GSA) to determine an optimal measurement configuration that provides the best measurement precision in optical scatterometry. Under each measurement configuration, the two determining factors of measurement precision are the corresponding noise level of measured signatures and the sensitivities of the profile parameters. GSA is used to study how the uncertainty in the model output can be apportioned to different sources of uncertainty in the model input variables [20]. We introduce the global sensitivity measure (termed the main effect) to evaluate the individual influence of an input profile parameter on the forward model output. This sensitivity measure is obtained by floating all the input profile parameters of interest simultaneously and then looking at the entire input space rather than at a particular point in that space; it thus overcomes the fatal limitation of LSA when the model input parameters are uncertain and the model is of unknown nonlinearity. By combining the corresponding noise level with the calculated main effect, we define a metric called the uncertainty index to evaluate the impact of random noise in measured signatures on the measurement precision for each measurement configuration. A configuration with a minimum uncertainty index is expected to result in the best measurement precision. We use the uncertainty index to determine an optimal measurement configuration in optical scatterometry.

The remainder of this paper is organized as follows. Section 2 introduces our definition of the uncertainty index and illustrates its method of calculation in detail. Section 3 provides the predictions made by the calculated uncertainty index and its comparisons with experimental and simulated results. Finally, we draw some conclusions in Section 4.

2. Method

2.1. Definition of the uncertainty index

In optical scatterometry, the forward model can be mathematically abstracted as

$$y = f(\mathbf{x}, \mathbf{a}). \tag{1}$$

Here, $\mathbf{x} = [x_1, x_2, \ldots, x_n]$ is a vector representing a set of n input profile parameters (e.g., CD, side wall angle, and height); $\mathbf{a} = [\varphi, \theta, \lambda]$ represents a measurement configuration defined as a combination of azimuthal angle φ, incidence angle θ, and wavelength λ; and y denotes the model output under the measurement configuration $\mathbf{a}$. For any structure under measurement, the actual dimensions of profile parameters are always uncertain or have certain variations that deviate from their nominal values. Assuming that the profile parameters of interest follow some distributions which are uniform or normal, the global sensitivity stands for the global variability of the model output over the entire range of input profile parameters. The global sensitivity measures, which are formulated as conditional variances, are often classified as variance-based, and are usually evaluated by the Monte Carlo technique or by the Latin hypercube sampling process. Under a measurement configuration $\mathbf{a}$, the total variance of the model output $V_i(y, \mathbf{a})$ for the ith input profile parameter x_i is defined as [20]:

$$V_i(y, \mathbf{a}) = E\left[V_{\mathbf{x}_{\sim i}}(y|x_i, \mathbf{a})\right] + V\left[E_{\mathbf{x}_{\sim i}}(y|x_i, \mathbf{a})\right], \tag{2}$$

where $\mathbf{x}_{\sim i}$ denotes a vector containing all input profile parameters but x_i. The first term in the right side of Eq. (2) represents the expectation of the conditional variances and is usually called the residual, while the second term represents the variance of the conditional expectations and is called the main effect:

$$M_i(\mathbf{a}) = V\left[E_{\mathbf{x}_{\sim i}}(y|x_i, \mathbf{a})\right]. \tag{3}$$

Here, the meaning behind the inner expectation operator is that the mean of y is taken over all possible values of $\mathbf{x}_{\sim i}$ while keeping x_i fixed, and the outer variance is taken over all possible values of x_i.

As a global sensitivity measure, the main effect can be utilized to evaluate the individual influence of an input profile parameter on the model output. A large main effect implies that the variations of an input profile parameter have a significant influence on the uncertainty of model output while all the profile parameters are floating simultaneously, and, inversely, the variations in model output will have a small impact on the uncertainty of that profile parameter. Thus, the main effect is an important factor in determining how the random noise in measured signatures impacts the profile parameters during the reconstructing procedure. In addition, another main factor is the measurement noise level σ (standard deviation), which is usually different for each configuration. By combining the main effects of each input profile parameter and the corresponding noise level, we define a metric called the uncertainty index to evaluate the impact of random noise in measured signatures on the precision of each measurement configuration. The uncertainty index for the ith profile parameter under a given measurement configuration $\mathbf{a}$ is defined as:

$$U_i(\mathbf{a}) = \frac{\sigma(\mathbf{a})}{M_i(\mathbf{a})}. \tag{4}$$

In general, a measurement configuration with the minimum uncertainty index is considered optimal, and it would result in the best measurement precision.

2.2. Calculation of the uncertainty index

As the noise level is mainly dependent on the instrument used and is easy to obtain, the difficulty is in deciding how to calculate the main effect for each profile parameter under a given measurement configuration. Currently, a number of GSA techniques can be used to calculate this sensitivity measure, such as those suggested by Morris [21], Sobol [22], and the extended Fourier amplitude sensitivity test (EFAST) method [23]. Due to its robustness, especially for a small sample size, and its high computational efficiency, the EFAST method is adopted. Its core feature is a flexible sampling scheme over the multidimensional space of input profile parameters, which is specified by a set of transformation functions [23]:

$$\hat{x}_i(s) = \frac{1}{2} + \frac{1}{\pi}\arcsin[\sin(\omega_i s + \phi_i)], \tag{5}$$

where $\hat{x}_i(s)$ is the normalized x_i as a function of s in the range of $[0, 1]$, s is a scalar variable varying over the range of $[-\pi, \pi]$, $\{\omega_i\}$ is a set of

Please cite this article as: Z. Dong, et al., Determination of an optimal measurement configuration in optical scatterometry using global sensitivity analysis, Thin Solid Films (2014), http://dx.doi.org/10.1016/j.tsf.2014.03.051

different angular frequencies associated with each parameter, and $\varnothing_i$ is a random phase shift chosen in [0, 2π).

The sampling scheme in Eq. (5) indicates that each of the input profile parameter x_i oscillates periodically at the corresponding frequency ω_i. If the ith input has a strong effect on the model output y, the oscillation of y at frequency ω_i will be of high amplitude. This is the fundamental rationale behind the EFAST method for calculating a sensitivity measure. The expectation of y can be approximated by

$$E(y) = \frac{1}{2\pi}\int_{-\pi}^{\pi} f[\hat{x}_1(s), \hat{x}_2(s), \ldots, \hat{x}_n(s)]ds = \frac{1}{2\pi}\int_{-\pi}^{\pi} f(s)ds, \tag{6}$$

Eq. (5) also indicates that the function $f(s) = f[\hat{x}_1(s), \hat{x}_2(s), \ldots, \hat{x}_n(s)]$ is a real-valued periodic function with a period of 2π, which can be expanded as a Fourier series

$$f(s) = \frac{a_0}{2} + \sum_{m=1}^{\infty}(a_m \cos ms + b_m \sin ms), \tag{7}$$

where a_m and b_m are the Fourier coefficients defined as

$$a_m = \frac{1}{\pi}\int_{-\pi}^{\pi} f(s)\cos msds, \tag{8a}$$

$$b_m = \frac{1}{\pi}\int_{-\pi}^{\pi} f(s)\sin msds, \tag{8b}$$

Consequently, we may calculate the total variance of the model output y as

$$V(y) = \frac{1}{2\pi}\int_{-\pi}^{\pi} f^2(s)ds - \left[\frac{1}{2\pi}\int_{-\pi}^{\pi} f(s)ds\right]^2 = \frac{1}{2}\sum_{m=1}^{\infty}\left(a_m^2 + b_m^2\right). \tag{9}$$

In fact, all the input profile parameters float simultaneously by sampling s in the interval of [−π, π]. Thus, a_m and b_m can be approximated as

$$a_m = \frac{2}{N_s}\sum_{k=1}^{N_s} f(s_k)\cos ms_k, \tag{10a}$$

$$b_m = \frac{2}{N_s}\sum_{k=1}^{N_s} f(s_k)\sin ms_k, \tag{10b}$$

where N_s is the sample size for the variable s. By evaluating the spectrum for the fundamental frequency ω_i and its higher harmonics $p\omega_i$ ($p = 1, 2, \ldots, \infty$), we may estimate the main effect of the ith input profile parameter x_i, i.e., the corresponding variance of y arising from the uncertainty of the ith input:

$$M_i = \frac{1}{2}\sum_{p=1}^{L}\left(a_{p\omega_i}^2 + b_{p\omega_i}^2\right). \tag{11}$$

Here, L is usually set as 4 or 6. When estimating the main effect of the ith input, a larger value of the ith fundamental frequency ω_i must be selected, while all other fundamental frequencies should be set relatively small in the range between 1 and $\omega_i/2L$ [23].

With the main effect calculated as in Eq. (11) and the corresponding noise level, we may estimate the uncertainty index of each profile parameter shown as in Eq. (4) for a given measurement configuration.

3. Results and discussions

3.1. Experimental setup

The experimental setup used in this work is a dual-rotating compensator Mueller matrix polarimeter (RC2®, J. A. Woollam Co.) with in-house forward modeling software based on rigorous coupled-wave analysis (RCWA) [5,24,25]. As schematically shown in Fig. 1, the system setting of the dual-rotating compensator Mueller matrix polarimeter in order of light propagation is $PC_{r1}SC_{r2}A$, where P and A stand for the fixed polarizer and analyzer, C_{r1} and Cr_2 refer to the 1st and 2nd frequency-coupled rotating compensators, and S stands for the sample [26,27]. With the light source used in this polarimeter, the wavelengths available are in the 193 to 1690 nm range, covering the spectral range of 400 to 800 nm used in this work. With this dual-rotating compensator setting, we can obtain the full 15 Mueller matrix elements of the sample under measurement, which are normalized by the first element.

The investigated sample is a one-dimensional Si grating whose SEM cross-section image is shown in Fig. 2. The etched Si grating is chosen for this study due to its long-term dimensional stability, higher refractive index contrast, and relevance to the semiconductor industry. Optical properties of Si are taken from Ref. [28]. As depicted in Fig. 2, the cross section of the Si grating is characterized by a symmetrical trapezoidal model with top critical dimension (TCD), grating height (Hgt), side-wall angle (SWA), and period (p). Nominal dimensions of the grating sample are $TCD = 360$ nm, $Hgt = 480$ nm, $SWA = 87°$, and $p = 800$ nm, while dimensions obtained from Fig. 2 are $TCD = 350$ nm, $Hgt = 472$ nm, and $SWA = 87.63°$.

In our experiments and numerical simulations, the model input is the three investigated profile parameters of the Si grating, including the *TCD*, the *Hgt*, and the *SWA*, while the grating period is fixed at its nominal dimension. The model output contains 15 Mueller matrix elements normalized by the first element. As mentioned in Section 2.1, the measurement configuration $\mathbf{a} = [\varphi, \theta, \lambda]$ is defined as a combination of azimuthal angle φ, incidence angle θ, and wavelength λ. As a simple example to demonstrate our GSA method, here we only determine an optimal azimuthal angle. In this case, the incidence angle is fixed at $\theta_0 = 65°$, the wavelength covers a fixed range of 400–800 nm, and the measurement configuration becomes a single variable of azimuthal angle, i.e., $\mathbf{a} = \varphi$, which varies in the range from 0° to 90° with a step of 5°. After taking into account all the 15 Mueller matrix elements and the wavelengths used, we define the uncertainty index of the ith profile parameter for a given azimuthal angle φ as

$$U_i(\phi) = \frac{1}{15K}\sum_{k=1}^{K}\sum_{n=1}^{15}\frac{\sigma_n(\phi, \theta_0, \lambda_k)}{M_{i,n}(\phi, \theta_0, \lambda_k)} \tag{12}$$

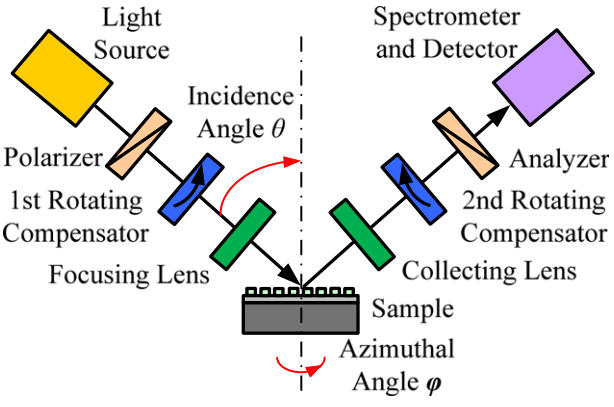

Fig. 1. Schematic of the dual-rotating compensator Mueller matrix polarimeter.

Please cite this article as: Z. Dong, et al., Determination of an optimal measurement configuration in optical scatterometry using global sensitivity analysis, Thin Solid Films (2014), http://dx.doi.org/10.1016/j.tsf.2014.03.051

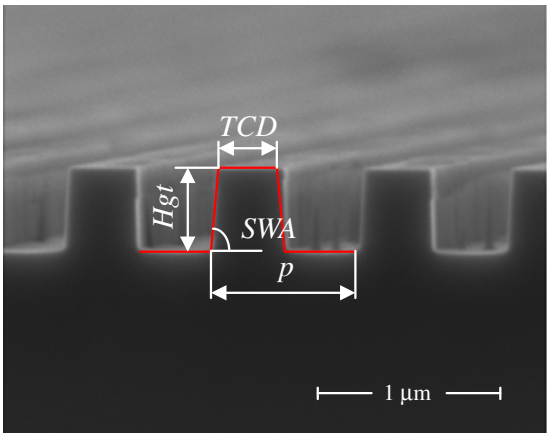

Fig. 2. SEM cross-section image of the investigated Si grating sample.

where $\sigma_n(\varnothing, \theta_0, \lambda_k)$ and $M_{i,n}(\varnothing, \theta_0, \lambda_k)$ are the noise level and the main effect for the given azimuthal angle φ (with the fixed incidence angle θ_0 and the kth wavelength λ_k) with the nth Mueller matrix element as the model output, respectively, and K is the number of wavelengths used. The noise levels (standard deviations) of the measured Mueller matrix can be estimated by the CompleteEASE™ software supplied with the polarimeter instrument. Fig. 3 shows the estimated noise levels of the Mueller matrix when measuring the investigated sample at an incidence angle of 65° and an azimuthal angle of 60°.

3.2. Experimental results

We calculated the main effects for each measurement configuration (i.e., azimuthal angle) by the EFAST method with a sample size of $Ns = 500$. We assume that the dimensions of the three input profile parameters under investigation followed a normal distribution with their standard deviations being about 2% of their nominal values. With the calculated main effects and the estimated noise levels provided by the polarimeter instrument, the uncertainty indices of the three profile parameters were obtained using Eq. (12) for each measurement configuration. Fig. 4 presents the normalized uncertainty indices of the three profile parameters. It is noted that different azimuthal angles show different uncertainty indices of the *TCD*, the *Hgt*, and the *SWA*. The minimum uncertainty indices of the three profile parameters are not located at the same position, and the optimal azimuthal angle with the best precision of profile parameters *TCD*, *Hgt*, and *SWA* should be 85°, 0°, and 85°, respectively.

To examine the predicted optimal measurement configuration, we performed experiments using the polarimeter instrument under different measurement configurations, i.e., at different azimuthal angles in the range from 0° to 90° with a step of 5°. For each azimuthal angle, 50 groups of the Mueller matrices with a spectral range of 400–800 nm were obtained using repeated measurements. The non-linear Levenberg–Marquardt (LM) algorithm was applied to reconstruct the profile parameters by fitting the measured Mueller matrices with the modeled ones [29], which converged very quickly to a minimum when a suitable initial condition was chosen. Each group of the measured Mueller matrices was fitted individually. Fig. 5 depicts the experimental uncertainties (using a 99.7% confidence interval) of the three reconstructed profile parameters. Comparing Fig. 4 with Fig. 5, we may observe the trend that the lower the uncertainty index, the better the precision of the reconstructed profile parameter. Importantly, the optimal measurement configurations with azimuthal angles of 85° and 0° predicted by the minimization of the uncertainty indices indeed result in the best experimental precision of *TCD* and *Hgt* respectively. However, the azimuthal angle of 85° predicted to be optimal for the reconstruction of *SWA* exhibits a slight deviation from the optimal angle of 90° obtained experimentally. It might be because the predictions make a compromise by considering all the dimensions around their nominal values. Another possible reason is the simplification of our forward model, which does not consider the thermal oxide layer on top of Si,

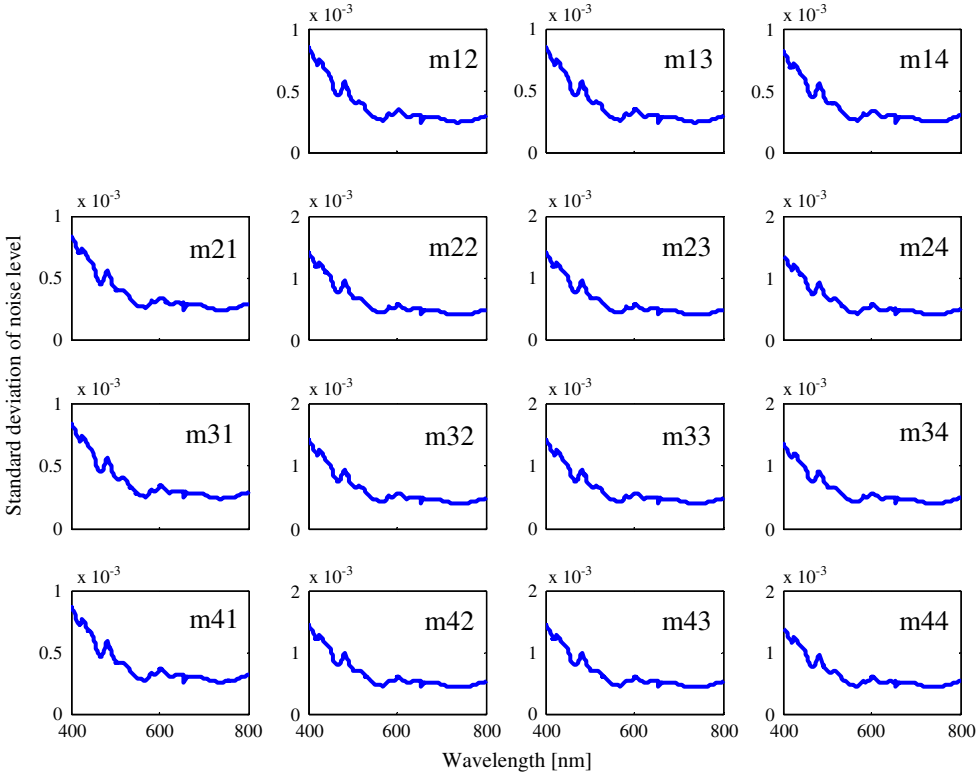

Fig. 3. Estimated noise levels of Mueller matrix elements by the polarimeter instrument when measuring the Si grating sample at an incidence angle of 65° and an azimuthal angle of 60°.

Please cite this article as: Z. Dong, et al., Determination of an optimal measurement configuration in optical scatterometry using global sensitivity analysis, Thin Solid Films (2014), http://dx.doi.org/10.1016/j.tsf.2014.03.051

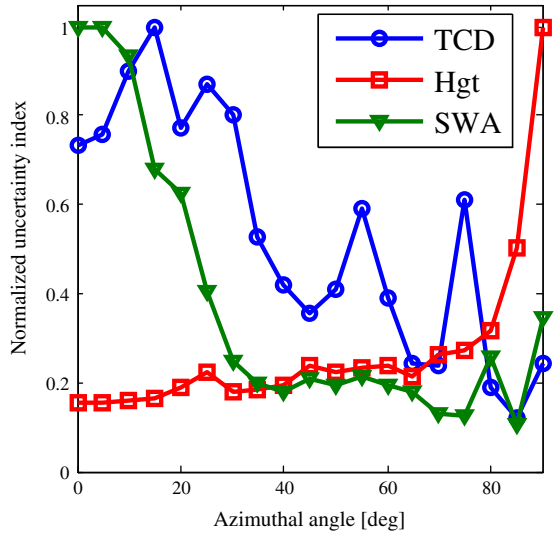

Fig. 4. Normalized uncertainty indices of *TCD*, *Hgt*, and *SWA* for the Si grating sample by the GSA method.

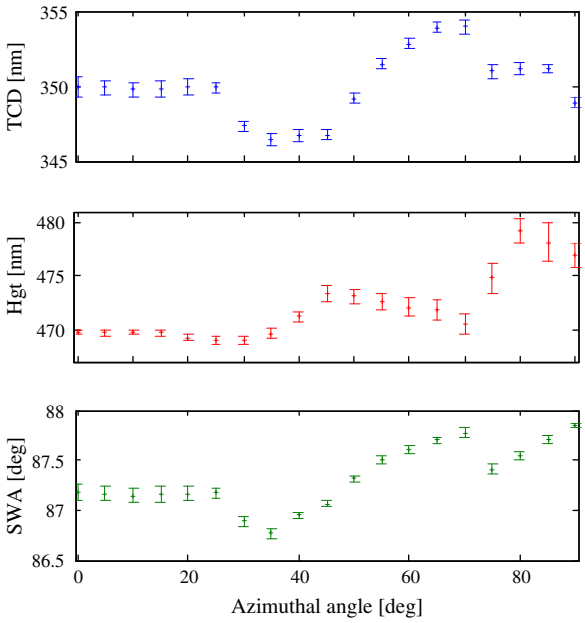

Fig. 6. Reconstructed results of *TCD*, *Hgt*, and *SWA* for the Si grating sample by the experiment, which include both the average values and the statistical uncertainties.

the roughness of the grating, and the rounded corners on the top and bottom of the structure.

Fig. 6 illustrates the reconstructed dimensions of the three profile parameters, including both the average values and the statistical uncertainties. It shows that the fitted parameters *TCD*, *Hgt* and *SWA* have a smooth and non-random dependence on the measurement azimuthal angle, which is probably caused by the non-uniformity of the grating periodicity, the simplification of the forward model, the truncation of the number of harmonics in the RCWA simulation, the numerical aperture of the focusing lens, and so on. Fig. 7 shows an example of the fitting result of both the calculated and the polarimeter-measured Mueller matrices at the incidence angle of 65° and the azimuthal angle of 30°; the reconstructed profile parameters are $TCD = 347.33 \pm 0.167$ nm, $Hgt = 468.96 \pm 0.201$ nm, and $SWA = 86.89 \pm 0.019°$. As observed from Fig. 7, the calculated Mueller matrix shows good agreement with the measured results. Consequently, we may conclude that the uncertainty index can be applied as the metric to determine an optimal measurement configuration for profile reconstruction in optical scatterometry.

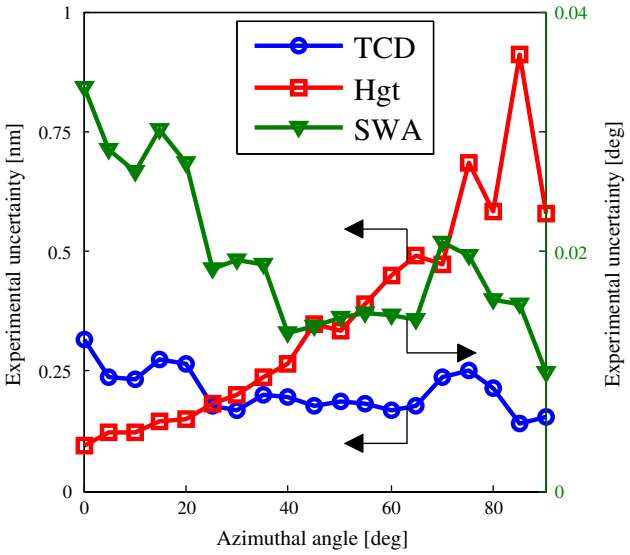

Fig. 5. Experimental uncertainties of *TCD*, *Hgt*, and *SWA* for the Si grating sample.

In addition, the current approach based on LSA [10,17,18] was also performed to determine the optimal measurement configuration for the investigated sample. The curvature matrix based on the partial derivatives of the modeled signatures with respect to the profile parameters at the nominal values over all measurement configurations was obtained by statistical analysis. The inverse of the curvature matrix was an estimate of the covariance matrix, and a minimization of the diagonal elements of the covariance matrix was used to determine the optimal measurement configuration when the objective function of the fitting algorithm is proportional to the Chi-square of the measured versus the modeled Mueller matrices. The LSA method also utilized the noise levels (standard deviations) of the Mueller matrix elements, which were obtained from the polarimeter instrument. The estimated uncertainties (using a 99.7% confidence interval) of the three profile parameters obtained by the LSA method are presented in Fig. 8. As shown in Figs. 5 and 8, the azimuthal angles of 85°, 20°, and 80° located at the minimum estimated uncertainty of *TCD*, *Hgt*, and *SWA*, respectively, are slightly different from the optimal angles of 85°, 0°, and 90° achieved by experiments. It might be because the reconstructed dimensions of the three profile parameters depicted in Fig. 6 deviate somewhat from their nominal values, while the partial derivative of a parameter is calculated with the other parameters fixed at their nominal values. However, there also appears to be a qualitative agreement, so that with a lower estimated uncertainty, the precision is better for the reconstructed profile parameter. These results indicate that both the uncertainty index by the proposed method and the estimated uncertainty by the LSA method can be applied as the metric to determine an optimal measurement configuration for a sample with its true dimensions close to its nominal values in optical scatterometry.

3.3. Comparison to the LSA method

To further explore the strength of the proposed method, we used the uncertainty index as the metric to determine an optimal measurement configuration for a set of Si grating samples with relatively large dimensional variation. In this case, the *TCD* ranges from 200 to 600 nm, the *Hgt* ranges from 300 to 700 nm, the *SWA* ranges from 75 to 90°, and the *p* is fixed at 800 nm. By considering all the possible samples, we assumed that the dimensions of the three input profile parameters under investigation followed a uniform distribution. With the same range of

Please cite this article as: Z. Dong, et al., Determination of an optimal measurement configuration in optical scatterometry using global sensitivity analysis, Thin Solid Films (2014), http://dx.doi.org/10.1016/j.tsf.2014.03.051

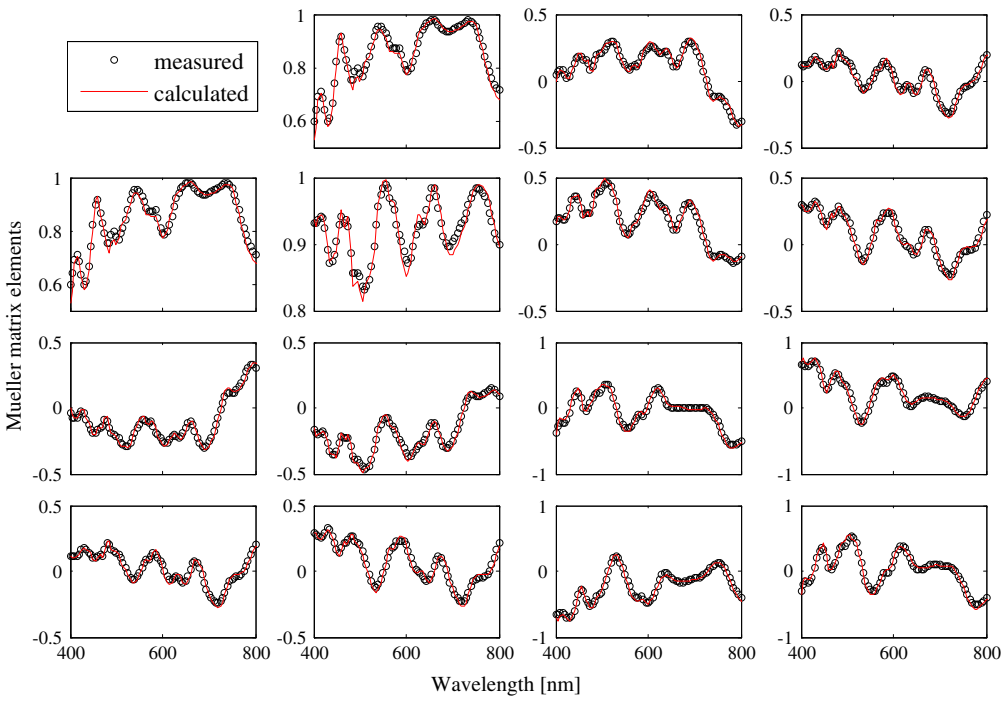

Fig. 7. Fitting result of the calculated and the polarimeter-measured Mueller matrices of the Si grating sample at an azimuthal angle of 30° and an incidence angle of 65°.

wavelengths, the incidence angle, and the sample size *Ns* described in Section 3.2, the normalized uncertainty indices of the three profile parameters are obtained and presented in Fig. 9. The optimal measurement configuration with the azimuthal angles of 50°, 40°, and 70° is predicted to be the optimal one for *TCD*, *Hgt*, and *SWA*, respectively, which is a compromise when considering all the possible gratings within the above dimensional distribution.

In order to examine the above prediction of the optimal measurement configuration, totally 30 Si grating samples were generated randomly to evaluate the precision of the three reconstructed profile parameters, and their measured Mueller matrixes were simulated by using rigorously modeled data with white noise. In this numerical simulation, the standard deviations of the white noise were also obtained from the polarimeter instrument, and the modeled data were calculated with the profile parameters fixed at their true values. The wavelengths used were also within a range from 400 to 800 nm, and the incidence angle was fixed at 65°. With each measurement configuration, 50 groups of measured Mueller matrixes were simulated for each grating sample. The non-linear LM algorithm was also utilized to reconstruct the profile parameters by fitting the simulated Mueller matrixes with the modeled ones. To achieve an optimal measurement configuration for all the samples, we calculated the relative uncertainty (with a 99.7% confidence interval) for each sample using its true dimension as a weight for each reconstructed parameter, and then obtained the mean relative uncertainty for all the 30 samples. Fig. 10 depicts the normalized mean relative uncertainty for each reconstructed parameter varying with the configuration (azimuthal angle). It is noted that the variation of the normalized mean relative uncertainty by numerical

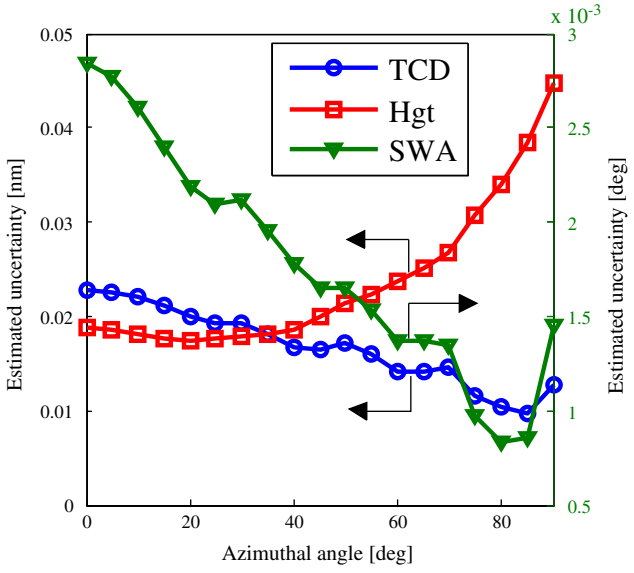

Fig. 8. Estimated uncertainties of *TCD*, *Hgt*, and *SWA* for the Si grating sample by the LSA method.

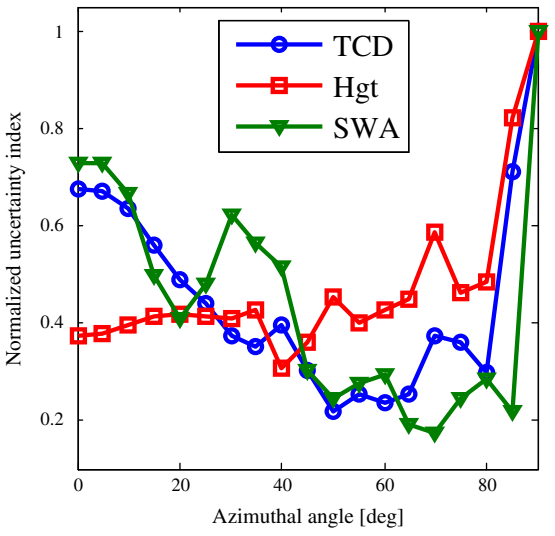

Fig. 9. Normalized uncertainty indices of *TCD*, *Hgt*, and *SWA* for a set of grating samples by the GSA method.

Please cite this article as: Z. Dong, et al., Determination of an optimal measurement configuration in optical scatterometry using global sensitivity analysis, Thin Solid Films (2014), http://dx.doi.org/10.1016/j.tsf.2014.03.051

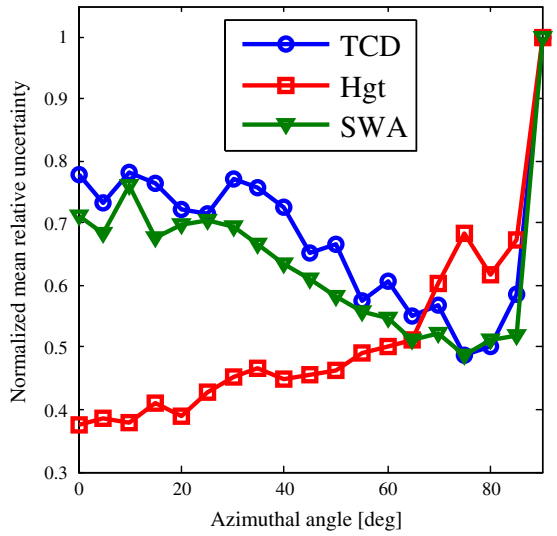

Fig. 10. Normalized mean relative uncertainties of 30 samples for *TCD*, *Hgt*, and *SWA* by numerical simulation.

simulation as shown in Fig. 10 is not in rigorous agreement with that of the normalized uncertainty index as depicted in Fig. 9. The optimal measurement configuration with azimuthal angles of 50°, 40°, and 70° is predicted to be optimal for the reconstructed profile parameters *TCD*, *Hgt*, and *SWA*, respectively, while the optimal angles obtained from numerical simulations are 75°, 10°, and 75°, respectively. This difference might be caused mainly by the finite number of samples, since the range of the investigated profile parameters is much larger. However, it does exhibit a qualitative agreement, in that the lower the uncertainty index, the better the mean precision of the 30 grating samples for the reconstructed profile parameters. Therefore, it suggests that the defined uncertainty index is suitable to determine an optimal measurement configuration for a set of samples with various dimensions.

The LSA method was also performed for the 30 samples. For example, Fig. 11 shows ten groups of the optimal azimuthal angles achieved by the minimization of the estimated uncertainty. In comparison with the results above, the optimal azimuthal angles with the lowest uncertainties of the reconstructed *TCD*, *Hgt*, and *SWA* are also shown in Fig. 11. For most samples, it shows an agreement between the optimal measurement configuration predicted by the LSA method and the optimal one achieved by numerical simulations. It is notable that the optimal azimuthal angle predicted by the LSA method varies significantly among the samples. This is because the LSA method is conducted by varying one profile parameter with a small offset from its nominal value and keeping the others fixed at their nominal values, and consequently the estimated uncertainty mainly measures the local effects of the profile parameters and significantly depends on the nominal dimensions of samples. This result implies that it is difficult to achieve a proper measurement configuration by the current LSA method for a set of samples with relatively large parameter variation.

4. Conclusions

In summary, we have proposed to apply GSA to determine an optimal measurement configuration for the best measurement precision in optical scatterometry. For each measurement configuration, we have defined a metric called the uncertainty index to evaluate the impact of random noise in measured signatures on the measurement precision by combining the global sensitivity measure, termed the main effect, with the corresponding noise level. For the grating sample with its true dimensions close to its nominal values, experiments performed with a dual-rotating compensator Mueller matrix polarimeter have

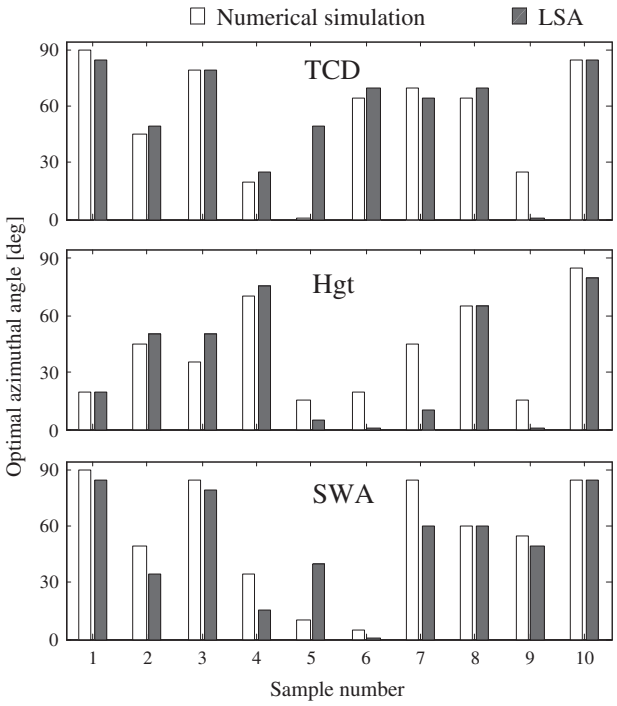

Fig. 11. Optimal azimuthal angles of 10 samples for *TCD*, *Hgt*, and *SWA* by the LSA method and numerical simulation.

shown an agreement between the theoretically predicted optimal configuration and the experimentally exhibited configuration.

For a set of grating samples with various dimensions, the GSA method can also predict an optimal measurement configuration, which deviates somewhat from the optimal ones resulting in the best precision from numerical simulations. However, it does show a qualitative agreement, in that the lower the uncertainty index, the better the mean precision of the samples for the reconstructed profile parameter. In contrast, the optimal configuration predicted using the LSA method is significantly dependent on the nominal dimensions of the samples, and consequently it is difficult to achieve a proper configuration for all the investigated samples. It thus suggests that the defined uncertainty index by the GSA method is suitable to determine the optimal measurement configuration, especially for a set of samples with relatively large dimensional variation.

Acknowledgments

The authors wish to acknowledge the financial support from the National Natural Science Foundation of China (Grant Nos. 91023032, 51005091, 51121002) and the National Instrument Development Specific Project of China (Grant No. 2011YQ160002). The authors would like to thank the unknown reviewers for their helpful comments and constructive suggestions that have improved the quality of the manuscript.

References

[1] C.J. Raymond, M.R. Murnane, S.L. Prins, S. Sohail, H. Naqvi, J.R. McNeil, J.W. Hosch, J. Vac. Sci. Technol. B 15 (1997) 361.
[2] H.T. Huang, W. Kong, F.L. Terry, Appl. Phys. Lett. 78 (2001) 3983.
[3] Y.N. Kim, J.S. Paek, S. Rabello, S. Lee, J. Hu, Z. Liu, Y. Hao, W. McGahan, Opt. Express 17 (2009) 21336.
[4] X.H. Niu, N. Jakatdar, J.W. Bao, C.J. Spanos, IEEE Trans. Semicond. Manuf. 14 (2001) 97.
[5] S.Y. Liu, Y. Ma, X.G. Chen, C.W. Zhang, Opt. Eng. 51 (2012) 081504.
[6] J.L. Zhu, S.Y. Liu, C.W. Zhang, X.G. Chen, Z.Q. Dong, J Micro Nanolithogr MEMS MOEMS 12 (2013) 013004.
[7] X.G. Chen, S.Y. Liu, C.W. Zhang, J.L. Zhu, Measurement 46 (2013) 2638.
[8] X.G. Chen, S.Y. Liu, C.W. Zhang, H. Jiang, Appl. Opt. 52 (2013) 6727.

Please cite this article as: Z. Dong, et al., Determination of an optimal measurement configuration in optical scatterometry using global sensitivity analysis, Thin Solid Films (2014), http://dx.doi.org/10.1016/j.tsf.2014.03.051

[9] X.G. Chen, S.Y. Liu, C.W. Zhang, H. Jiang, J Micro Nanolithogr MEMS MOEMS 12 (2013) 033013.
[10] P.C. Logofătu, Appl. Opt. 41 (2002) 7179.
[11] H. Gross, A. Rathsfeld, Waves Random Complex Media 18 (2008) 129.
[12] A. Saltelli, S. Taratola, F. Campolongo, Sensitivity Analysis in Practice, A Guide to Assessing Scientific Models, John Willey & Sons Ltd, New York NY, 2004.
[13] Y.S. Ku, S.C. Wang, D.M. Shyu, N. Smith, Opt. Express 14 (2006) 8482.
[14] P.C. Logofătu, Appl. Opt. 41 (2002) 7187.
[15] R. Silver, T. Germer, R. Attota, B.M. Barnes, B. Bunday, J. Allgair, E. Marx, J. Jun, Proc. SPIE 6518 (2007) 65180U.
[16] M. Foldyna, A. De Martino, E. Garcia-Caurel, R. Ossikovski, C. Licitra, F. Bertin, K. Postava, B. Drevillon, Eur. Phys. J. Appl. Phys. 42 (2008) 351.
[17] T.A. Germer, H.J. Patrick, R.M. Silver, B. Bunday, Proc. SPIE 7272 (2009) 72720T.
[18] P. Vagos, J. Hu, Z. Liu, S. Rabello, Proc. SPIE 7272 (2009) 72721N.
[19] A. Saltelli, P. Annoni, I. Azzini, F. Campolongo, M. Saisana, S. Tarantola, Comput. Phys. Commun. 181 (2010) 259.
[20] A. Saltelli, M. Ratto, T. Andres, F. Campolongo, J. Cariboni, D. Gatelli, M. Saisana, S. Tarantola, Global Sensitivity Analysis: The Primer, John Wiley & Sons Ltd, New York NY, 2008.
[21] M.D. Morris, Technometrics 33 (1991) 161.
[22] I.M. Sobol, Yu.L. Levitan, Comput. Phys. Commun. 117 (1999) 52.
[23] A. Saltelli, S. Tarantola, K.P.S. Chan, Technometrics 41 (1999) 39.
[24] M.G. Moharam, E.B. Grann, D.A. Pommet, T.K. Gaylord, J. Opt. Soc. Am. A 12 (1995) 1068.
[25] L. Li, J. Opt. Soc. Am. A 13 (1996) 1870.
[26] R.W. Collins, J. Koh, J. Opt. Soc. Am. A 16 (1999) 1997.
[27] C. Chen, I. An, G.M. Ferreira, N.J. Podraza, J.A. Zapien, R.W. Collins, Thin Solid Films 455–456 (2004) 14.
[28] C.M. Herzinger, B. Johs, W.A. McGahan, J.A. Woollam, W. Paulson, J. Appl. Phys. 83 (1998) 3323.
[29] C.W. Zhang, S.Y. Liu, T.L. Shi, Z.R. Tang, J. Opt. Soc. Am. A 26 (2009) 2327

Please cite this article as: Z. Dong, et al., Determination of an optimal measurement configuration in optical scatterometry using global sensitivity analysis, Thin Solid Films (2014), http://dx.doi.org/10.1016/j.tsf.2014.03.051